

Current experimental constraints on the next-to-minimal supersymmetric standard model with large λ

Junjie Cao¹ and Jin Min Yang²¹*Ottawa-Carleton Institute for Physics, Department of Physics, Carleton University, Ottawa, Canada K1S 5B6*²*Institute of Theoretical Physics and Kavli Institute for Theoretical Physics China, Academia Sinica, Beijing 100190, China*
(Received 7 October 2008; published 1 December 2008)

The next-to-minimal supersymmetric standard model (NMSSM) with a large λ (the mixing parameter between the singlet and doublet Higgs fields) is well motivated since it can significantly push up the upper bound on the standard model-like Higgs boson mass to solve the little hierarchy problem. In this work we examine the current experimental constraints on the NMSSM with a large λ , which include the direct search for Higgs bosons and sparticles at colliders, the indirect constraints from precision electroweak measurements, the cosmic dark matter relic density, the muon anomalous magnetic moment, as well as the stability of the Higgs potential. We find that, with the increase of λ , parameters like $\tan\beta$, M_A , μ , and M_2 are becoming more stringently constrained. It turns out that the maximal reach of λ is limited by the muon anomalous magnetic moment, and for smuon masses of 200 GeV (500 GeV) the parameter space with $\lambda \gtrsim 1.5(0.6)$ is excluded.

DOI: 10.1103/PhysRevD.78.115001

PACS numbers: 14.80.Cp, 11.30.Qc, 12.60.Fr

I. INTRODUCTION

Since the minimal supersymmetric standard model (MSSM) [1] suffers from the μ problem [2] and the little hierarchy problem, some nonminimal supersymmetric models have recently attracted much attention, among which the most intensively studied is the next-to-minimal supersymmetric standard model (NMSSM) [3]. In the NMSSM there is no dimensionful parameters in the supersymmetry (SUSY)-conserving sector and the μ term is dynamically generated through the coupling between the two Higgs doublets and a newly introduced singlet Higgs field which develops a vacuum expectation value of the order of the SUSY breaking scale. The NMSSM provides two ways to alleviate the little hierarchy problem. One is to relax the LEP II lower bound on the mass of the standard model (SM)-like Higgs boson, h , by diluting ZZh coupling through the singlet component of h and/or by suppressing the visible decay $h \rightarrow b\bar{b}$ by introducing the new decay of h [4]. The other is to push up the Higgs boson mass with a large λ , which can be seen from the tree-level upper bound of the Higgs boson mass [5],

$$m_{h,\max}^2 \simeq m_Z^2 \cos^2 2\beta + \lambda^2 v^2 \sin^2 2\beta \quad (1)$$

where $\tan\beta = \langle H_u \rangle / \langle H_d \rangle$, $v^2 = \langle H_u \rangle^2 + \langle H_d \rangle^2$, and λ is the mixing parameter between the singlet and doublet Higgs fields defined in Eq. (2).

Note that the choice of a large λ to solve the little hierarchy problem may be limited by the perturbativity of the theory at the scale Λ since the value of λ is increasing with the energy scale [6]. If this scale Λ is the grand unified theory (GUT) scale, λ should be less than about 0.7 at the weak scale, leading to an upper bound on the Higgs boson mass of about 150 GeV [5]. However, the bound on λ from the perturbativity consideration can be relaxed by

embedding the NMSSM in some more complex frameworks. For example, in the fat Higgs model [7], by completing the NMSSM (or NMSSM-like models) with an appropriate strong dynamics at an intermediate scale (much lower than the GUT scale), λ can be as large as 2 at the weak scale and the Higgs boson mass can be pushed up to about 400 GeV. In this work, regardless of the detailed forms of the ultraviolet physics, we treat the NMSSM as an effective theory and examine the current experimental constraints on its parameter space.

Such phenomenological studies on the Higgs boson and supersymmetry are pressing since the mystery of the Higgs sector will be unveiled at the LHC in the near future. If the SM-like Higgs boson is discovered with a mass above the MSSM upper bound, the NMSSM (or other NMSSM-like models) with a large λ , generally called λ SUSY [8], will be immediately favored since it not only inherits all the advantages of the MSSM, such as unifying gauge couplings and providing a dark matter candidate, but also is free from the μ problem and the little hierarchy problem. For the phenomenological studies of these models, a primary work is to examine the current experimental constraints on their parameter space.

We note that various constraints on the NMSSM have been studied in the literature, but different constraints were considered in different papers. For example, in [9] the authors mainly considered the LEP II constraints and put emphasize on the small λ case. The package NMSSMTOOLS [10] encoded various constraints (like the LEP II searches for the Higgs boson, cosmic dark matter, and the stability of the Higgs potential), but it is still not complete since it does not include the indirect constraints from precision electroweak measurements and the muon anomalous magnetic moment. In this work we consider all these constraints and especially focus on the case with a large λ .

As will be shown from our study, with the increase of λ , the parameter space gets more stringently constrained. Figuring out the allowed parameter space is helpful for exploring such low energy supersymmetry at the LHC and also may shed some light on constructing the ultraviolet physics from the bottom-up view.

This paper is organized as follows. In Sec. II we briefly describe the structure of the NMSSM with emphasis on its difference from the MSSM. In Sec. III we summarize the constraints considered in this work and briefly discuss their characters. In Sec. IV we scan over the NMSSM parameter space and display the region allowed by all these constraints. In Sec. V we give our conclusions.

II. ABOUT THE NMSSM

The NMSSM extends the matter fields of the MSSM by adding one gauge singlet superfield \hat{S} , and its superpotential takes the form [3]

$$W = \lambda \varepsilon_{ij} \hat{H}_u^i \hat{H}_d^j \hat{S} + \frac{1}{3} \kappa \hat{S}^3 + Y_u \varepsilon_{ij} \hat{Q}^i \hat{U} \hat{H}_u^j - Y_d \varepsilon_{ij} \hat{Q}^i \hat{D} \hat{H}_d^j - Y_e \varepsilon_{ij} \hat{L}^i \hat{E} \hat{H}_d^j \quad (2)$$

where \hat{Q} , \hat{U} , and \hat{D} are squark superfields, \hat{L} and \hat{E} are slepton superfields, and \hat{H}_u and \hat{H}_d are Higgs doublet superfields. The soft SUSY breaking terms are given by

$$\begin{aligned} V_{\text{soft}} = & \frac{1}{2} M_2 \lambda^a \lambda^a + \frac{1}{2} M_1 \lambda' \lambda' + m_d^2 |H_d|^2 + m_u^2 |H_u|^2 \\ & + m_S^2 |S|^2 + m_Q^2 |\tilde{Q}|^2 + m_U^2 |\tilde{U}|^2 + m_D^2 |\tilde{D}|^2 \\ & + m_L^2 |\tilde{L}|^2 + m_E^2 |\tilde{E}|^2 + (\lambda A_\lambda \varepsilon_{ij} H_u^i H_d^j S + \text{H.c.}) \\ & - (\frac{1}{3} A_\kappa S^3 + \text{H.c.}) + (Y_u A_U \varepsilon_{ij} \tilde{Q}^i \tilde{U} H_u^j \\ & - Y_d A_D \varepsilon_{ij} \tilde{Q}^i \tilde{D} H_d^j - Y_e A_E \varepsilon_{ij} \tilde{L}^i \tilde{E} H_d^j + \text{H.c.}) \quad (3) \end{aligned}$$

Note that just like the MSSM, the NMSSM has the feature that SUSY breaking induces the electroweak symmetry breaking. Before SUSY breaking (i.e. without the soft breaking terms), the Higgs scalars have zero vacuum expectation values (vevs) in the supersymmetric vacuum of the scalar potential, and thus the electroweak symmetry is not broken. After SUSY breaking (i.e. with the soft breaking terms), the Higgs scalars develop nonzero vevs in the physical (nonsupersymmetric) vacuum of the scalar potential, and hence the electroweak symmetry is spontaneously broken and the μ parameter is generated, $\mu = \lambda \langle S \rangle$. Since both the electroweak symmetry breaking and the μ parameter generation are induced by SUSY breaking, their scales should naturally be at the SUSY breaking scale (the scale of soft breaking mass parameters).

The differences of the NMSSM and MSSM come from the Higgs sector and the neutralino sector [3]. In the Higgs sector of the NMSSM there are three CP -even and two CP -odd Higgs bosons. In the basis $[\text{Re}(H_u^0), \text{Re}(H_d^0), \text{Re}(S)]$, the mass-squared matrix elements for CP -even Higgs bosons are

$$\mathcal{M}_{S,11}^2 = m_A^2 \cos^2 \beta + m_Z^2 \sin^2 \beta, \quad (4)$$

$$\mathcal{M}_{S,22}^2 = m_A^2 \sin^2 \beta + m_Z^2 \cos^2 \beta, \quad (5)$$

$$\begin{aligned} \mathcal{M}_{S,33}^2 = & \frac{\lambda^2 v^2}{4\mu^2} m_A^2 \sin^2 2\beta - \frac{\lambda \kappa}{2} v^2 \sin 2\beta \\ & + \frac{1}{\lambda^2} \mu (4\kappa^2 \mu - \lambda A_\kappa), \quad (6) \end{aligned}$$

$$\mathcal{M}_{S,12}^2 = (2\lambda^2 v^2 - m_Z^2 - m_A^2) \sin \beta \cos \beta, \quad (7)$$

$$\mathcal{M}_{S,13}^2 = 2\lambda \mu v \sin \beta - \frac{\lambda v}{2\mu} m_A^2 \sin 2\beta \cos \beta - \kappa \mu v \cos \beta, \quad (8)$$

$$\mathcal{M}_{S,23}^2 = 2\lambda \mu v \cos \beta - \frac{\lambda v}{2\mu} m_A^2 \sin \beta \sin 2\beta - \kappa \mu v \sin \beta. \quad (9)$$

In the basis $[\tilde{A}, \text{Im}(S)]$ with $\tilde{A} = \cos \beta \text{Im}(H_u^0) + \sin \beta \text{Im}(H_d^0)$, the mass-squared matrix elements for the CP -odd Higgs bosons are

$$\mathcal{M}_{P,11}^2 = \frac{2\mu}{\sin 2\beta} \frac{\lambda A_\lambda + \kappa \mu}{\lambda} \equiv m_A^2, \quad (10)$$

$$\mathcal{M}_{P,22}^2 = \frac{3}{2} \lambda \kappa v^2 \sin 2\beta + \frac{\lambda^2 v^2}{4\mu^2} m_A^2 \sin^2 2\beta + \frac{3}{\lambda} \mu A_\kappa, \quad (11)$$

$$\mathcal{M}_{P,12}^2 = \frac{\lambda v}{2\mu} m_A^2 \sin 2\beta - 3\kappa \mu v. \quad (12)$$

As shown in Eq. (10), we can choose m_A instead of A_λ as a free parameter. So compared with the MSSM, the NMSSM has three additional parameters: λ , κ , and A_κ . Conventionally, λ is chosen to be positive while κ and A_κ can be either positive or negative. Note that Eqs. (9) and (12) indicate that the parameters λ and $\kappa \mu$ affect the mixings between doublet and singlet Higgs fields, while A_κ only affects the squared mass of the singlet Higgs field.

In the neutralino sector, the NMSSM predicts one extra neutralino. In the basis $(-i\lambda_1, -i\lambda_2, \psi_u^0, \psi_d^0, \psi_s)$ the neutralino mass matrix is given by [3]

$$\begin{pmatrix} M_1 & 0 & m_Z \sin \theta_W \sin \beta & -m_Z \sin \theta_W \cos \beta & 0 \\ M_2 & -m_Z \cos \theta_W \sin \beta & m_Z \cos \theta_W \cos \beta & 0 & 0 \\ & 0 & & -\mu & -\lambda v \cos \beta \\ & & & 0 & -\lambda v \sin \beta \\ & & & & 2\frac{\kappa}{\lambda} \mu \end{pmatrix}. \quad (13)$$

This mass matrix is independent of A_κ , and the role of λ is to introduce the mixings of ψ_s with ψ_u^0 and ψ_d^0 , and $\kappa \mu$ is to affect the mass of ψ_s . From Eqs. (9), (12), and (13), one

can learn that in the limit $\lambda, \kappa \rightarrow 0$, the singlet field has no mixing with the doublet field and thus is decoupled. In this case, the NMSSM can recover the MSSM.

III. CONSTRAINTS ON THE NMSSM PARAMETERS

Before we proceed to discuss experimental constraints on the parameters of the NMSSM, we take a look at the bounds on λ and κ from the requirement that the theory should stay perturbative under a certain scale Λ . The renormalization group equations (RGEs) for λ and κ under the scale Λ take the following form [11]:

$$\frac{d\lambda}{d\ln\mu} = \frac{\lambda}{16\pi^2} (4\lambda^2 + 2\kappa^2 + 3Y_t^2 + 3Y_b^2 + Y_\tau^2 - 3g^2 - g'^2), \quad (14)$$

$$\frac{d\kappa}{d\ln\mu} = \frac{6\kappa}{16\pi^2} (\lambda^2 + \kappa^2), \quad (15)$$

where g and g' are the $SU(2)_L$ and $U(1)_Y$ gauge couplings. These RGEs indicate that the values of λ and κ increase with the energy scale. The requirement of perturbativity till the cutoff scale Λ , i.e., $\lambda(\Lambda) \leq 2\pi$ and $\kappa(\Lambda) \leq 2\pi$, will set upper bounds on λ and κ at the weak scale (throughout this paper, all input parameters are defined at the weak scale unless otherwise specified). For example, if we assume that new dynamics appears at $\Lambda = 10$ TeV, we get $\lambda^2 + \kappa^2 \leq 4.2$, and for $\lambda > 1.5$, κ must be less than 1.2; however, if Λ is chosen to be the GUT scale, a stringent bound $\lambda^2 + \kappa^2 \leq 0.5$ is obtained [6]. In our following numerical study we let λ and κ vary below 2 and 1, respectively, and this corresponds to setting $\Lambda \simeq 10$ TeV.

In our study we consider the following constraints on the parameters of the NMSSM:

- (1) Constraints on the neutralino and chargino sectors, which include the following: the bound from invisible Z decay $\Gamma(Z \rightarrow \chi_1^0 \chi_1^0) < 1.76$ MeV; the upper bounds on neutralino pair productions at LEP II, $\sigma(e^+ e^- \rightarrow \chi_1^0 \chi_i^0) < 10^{-2}$ pb ($i > 1$) and $\sigma(e^+ e^- \rightarrow \chi_i^0 \chi_j^0) < 10^{-1}$ pb; and the LEP II bound on the lightest chargino mass $m_{\chi_1^\pm} > 103.5$ GeV. These bounds will mainly constrain the parameters M_1, M_2 , and μ .
- (2) Lower bounds on sparticle masses from LEP and Tevatron experiments [12]:

$$\begin{aligned} m_{\tilde{e}} &> 73 \text{ GeV}, & m_{\tilde{\mu}} &> 94 \text{ GeV}, \\ m_{\tilde{\tau}} &> 81.9 \text{ GeV}, & m_{\tilde{q}} &> 250 \text{ GeV}, \\ m_{\tilde{l}} &> 89 \text{ GeV}, & m_{\tilde{b}} &> 95.7 \text{ GeV}, \\ m_{\tilde{g}} &> 195 \text{ GeV}, \end{aligned}$$

where $m_{\tilde{q}}$ denotes the masses for the first two-generation squarks. These constraints will put lower

bounds on the soft breaking masses for sleptons and squarks.

- (3) The LEP II lower bound on the charged Higgs boson mass, $m_{H^\pm} > 78.6$ GeV, which gives a lower bound on m_A through the relation $m_{H^\pm}^2 = m_A^2 + M_W^2 - \frac{1}{2}\lambda^2 v^2$.
- (4) Constraints from the direct search for the Higgs boson at LEP II [13], which include various channels of Higgs boson production [10]. They will constrain the parameters $m_A, \tan\beta, \lambda$, as well as the masses and the chiral mixing of top squarks in a complex way.
- (5) Constraints from the relic density of cosmic dark matter, i.e. $0.0945 < \Omega h^2 < 0.1287$ [14], assuming the lightest neutralino is the dark matter particle. The relic density will constrain the parameters $M_1, M_2, \mu, m_A, \tan\beta$, and λ in a complex way [15].
- (6) Constraints from the stability of the Higgs potential, which requires that the physical vacuum of the Higgs potential with nonvanishing vevs of Higgs scalars should be lower than any local minima. Also, the scale of the Higgs soft breaking parameters should not be much higher than the electroweak scale to avoid the fine-tuning problem. Here we set 1 TeV as the upper bound of the soft breaking parameters in the Higgs sector. This will constrain the parameters $m_A, \mu, A_\kappa, \lambda$, and $\tan\beta$.
- (7) Constraints from precision electroweak observables such as $\rho_{\text{lept}}, \sin^2\theta_{\text{eff}}^{\text{lept}}$, and M_W , or their combinations $\epsilon_i (i = 1, 2, 3)$ [16]. We require the predicted ϵ_i in the NMSSM to be compatible with the LEP/SLD data at the 95.6% confidence level or, equivalently, $\chi^2/\text{dof} \leq 8.1/3$. We take the correlation coefficient of ϵ_i from [17] in calculating χ^2 . This requirement will constrain the parameters $\tan\beta, m_A$, as well as the soft breaking parameters in the third generation squark sector.
- (8) Constraints from $R_b = \Gamma(Z \rightarrow \bar{b}b)/\Gamma(Z \rightarrow \text{hadrons})$, whose measured value is $R_b^{\text{exp}} = 0.21629 \pm 0.00066$. The SM prediction is $R_b^{\text{SM}} = 0.21578$ for $m_t = 173$ GeV [12]. In our analysis we require that R_b^{SUSY} is within the 2σ range of its experimental value. It has been shown that the SUSY contribution to R_b might be sizable for large $\tan\beta$ [18].
- (9) Constraints from the muon anomalous magnetic moment a_μ . Now both the theoretical prediction and the experimental measurement of a_μ have reached a remarkable precision, but they show a significant deviation, $a_\mu^{\text{exp}} - a_\mu^{\text{SM}} = (29.5 \pm 8.8) \times 10^{-10}$ [19]. In our analysis we require the SUSY effects to account for such a deviation at the 2σ level. The character of the SUSY contribution to a_μ is that it is suppressed by smuon masses but enhanced by $\tan\beta$.

Among the above constraints, (1)–(6) and (9) have been encoded in the package NMSSMTOOLS [10]. In our calculations we extend it by including the constraints (7) and (8).

The analytic expressions of ϵ_i and R_b in the NMSSM were given in our recent work [18]. In [18] we also calculated the NMSSM contribution to a_μ (when we started that work, the results in [20,21] had not yet been published), where we extended the neutralino- and chargino-mediated MSSM contributions [22] to the NMSSM and also considered the contributions from the Higgs-mediated diagrams [23] and from the Barr-Zee diagrams [24]. We checked that our a_μ results in [18] agree with those in [20].

Note that in our analysis we did not include the constraints from various B decays [25] because they are dependent on squark flavor mixings and thus involve additional parameters.

IV. ALLOWED REGIONS OF THE NMSSM PARAMETERS

In this section, we scan over the NMSSM parameter space to look for the region allowed by the constraints in the preceding section. Since we are interested in the parameters sensitive to the constraints, we make some assumptions (as conservative as possible) for the other parameters such as soft breaking parameters in squark, slepton, and gaugino sectors.

For the parameters in the squark sector, we assume the so-called m_h^{\max} scenario, which can maximize the lightest Higgs boson mass [26]. This scenario assumes all the soft breaking masses in the squark sector to be degenerate,

$$M_{\tilde{q}} = M_{\tilde{Q}_i} = M_{U_i} = M_{D_i} \quad (16)$$

with i being the generation index. It also assumes the trilinear couplings to be degenerate, $A_{u_i} = A_{d_i}$ with $(A_{u_i} - \mu \cot\beta)/M_{\tilde{q}} = 2$. We fix $M_{\tilde{q}} = 1$ TeV in our analysis since large $M_{\tilde{q}}$ can not only enhance the lightest Higgs boson mass, but also decrease the contribution of the third generation squarks to the electroweak parameters, which has the same sign as the Higgs contributions [8]. For the parameters in the slepton sector, we note that the slepton masses have little effect on the constraints, except for the muon anomalous magnetic moment. In our calculation we assume all the soft breaking parameters in the slepton sector are degenerate and take a value of 200 GeV (we will discuss the effects of its variation). For the gaugino mass parameters, we assume the grand unification relation $M_1 = \frac{5}{3}(g'^2/g^2)M_2$.

With the above assumptions, the free parameters are reduced to seven ($\lambda, \kappa, A_\kappa, \tan\beta, m_A, \mu, M_2$) and are within the capability of our computer to perform a scan. During our scan, we first divide the varying range of λ into bins, with each bin width being 0.1, and then we vary the values of other parameters in the following ranges:

$$\begin{aligned} -1 &\leq \kappa \leq 1, \\ 1 &\leq \tan\beta \leq 60, \\ -1 \text{ TeV} &\leq A_\kappa < 1 \text{ TeV}, \\ 50 \text{ GeV} &\leq m_A, \mu, M_2 \leq 1 \text{ TeV}. \end{aligned} \quad (17)$$

With 2×10^8 samples in each bin and keeping the points satisfying the constraints, we finally get the allowed regions of these parameters. Our scan results indicate that the number of samples that survived for $\lambda < 0.5$ is much larger than that for $\lambda > 0.5$, which means that the parameters for small λ are much less constrained than the case with large λ . Since we are interested in large λ , here we only show our scan results for $\lambda > 0.5$.

In Fig. 1 we display the parameters (scatter plots) satisfying all the constraints (1)–(9) in the plane of λ versus $\tan\beta$. Also, we present a curve which is the upper bound on $\tan\beta$ without considering the muon g-2 constraints. To get this curve, we fix λ and scan over the parameters in Eq. (17). We adopt the important sampling method [27] to optimize the varying range of $\tan\beta$.

Figure 1 shows that the upper bound on $\tan\beta$ gets stronger as λ gets large, and when all the constraints are considered, λ is upper bounded by about 1.5. The underlying reason for this is that the constraints (1)–(8), especially the constraint (7), have limited the maximal value of $\tan\beta$, which decreases with the increase of λ . Since a large

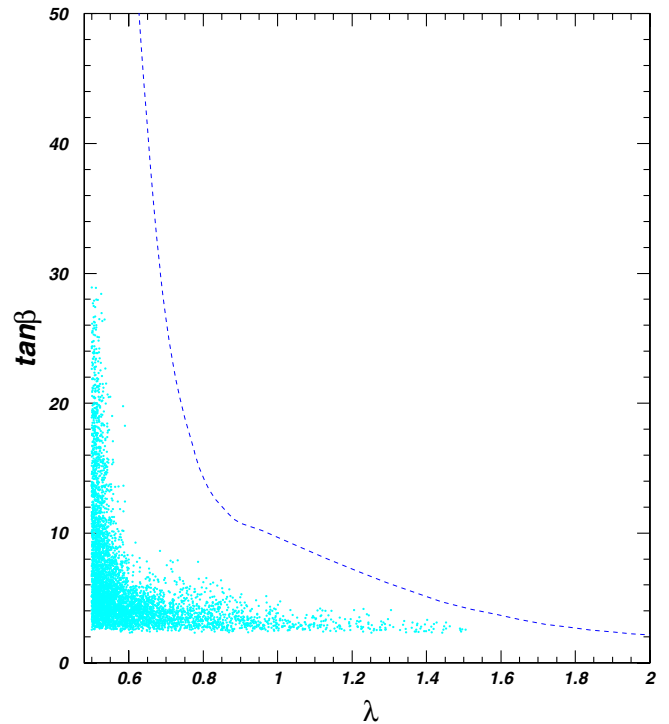


FIG. 1 (color online). The scatter plots are the NMSSM parameters satisfying all the constraints (1)–(9). The curve is the upper bound on $\tan\beta$ without considering the muon g-2 constraints.

$\tan\beta$ is needed to explain the deviation of the muon $g-2$, λ must terminate at a certain value where the corresponding $\tan\beta$ value is too small to explain the muon $g-2$. We have checked that the maximal value of λ is dependent on the slepton mass. For example, for slepton masses of 100 GeV, 280 GeV, and 500 GeV, the bounds on λ are $\lambda \lesssim 2$, $\lambda \lesssim 1$, and $\lambda \lesssim 0.6$, respectively.

In Fig. 2 we display the NMSSM parameters satisfying all the constraints in different planes. We see that for a large λ the parameters m_A , μ , M_2 , and A_κ are also bounded in a certain region. For $\lambda = 1$, these bounded regions are $400 \text{ GeV} \lesssim m_A \lesssim 800 \text{ GeV}$, $150 \text{ GeV} \lesssim \mu \lesssim 250 \text{ GeV}$, $150 \text{ GeV} \lesssim M_2 \lesssim 300 \text{ GeV}$, and $A_\kappa \lesssim 600 \text{ GeV}$.

From the plot of M_A versus λ in Fig. 2, one can see that the lower bound of M_A increases as λ becomes large. The reason is that the LEP II direct search for the Higgs boson mainly limits the mass and the couplings of the light CP -even Higgs boson whose component is dominated by the doublet Higgs field H_u or H_d . For $\tan\beta > 1$, this Higgs boson should be dominantly composed from the H_u field since $\mathcal{M}_{S,11}^2$ is smaller than $\mathcal{M}_{S,22}^2$, and its mass is to be reduced by the off-diagonal elements $\mathcal{M}_{S,12}^2$ and $\mathcal{M}_{S,13}^2$. As λ gets larger, these off-diagonal elements get larger and hence reduce the mass of the light CP -even Higgs boson, which then requires a larger M_A to compensate in order to satisfy the LEP II lower bound.

The plot of μ versus λ in Fig. 2 indicates that, with the increase of λ , the upper bound of μ decreases. This is because in the off-diagonal elements $\mathcal{M}_{S,13}^2$ and $\mathcal{M}_{S,23}^2$

(which reduce the light CP -even Higgs boson mass), λ is always associated with μ , and to meet the LEP II bound, a large λ must be accompanied by a small μ .

The plot of M_2 versus λ in Fig. 2 shows that M_2 is also bounded in a narrow region. This is because the relic density of dark matter correlates the parameters m_A , μ , M_2 , λ , and $\tan\beta$ in a complex way, and a large value for any of these parameters will limit severely the region of other parameters.

The plot of A_κ versus λ in Fig. 2 shows that the trilinear soft breaking parameter A_κ for the singlet field is also limited. This can be understood from the expressions of $\mathcal{M}_{S,33}^2$ and $\mathcal{M}_{P,22}^2$. The stability of the Higgs potential requires both of them to be positive, which sets a double-sided bound on A_κ .

We also studied the relationship between the Yukawa couplings λ and κ , and we found no correlation between them. Even for $\lambda = 1.5$, the value of κ can still vary from 0.3 to 1.

Next, we take a look at the Higgs boson masses allowed by the constraints. Since a large λ can enhance the lightest CP -even Higgs boson mass and thus avoid the little hierarchy problem, it is interesting to look at the dependence of the Higgs boson masses on the parameter λ .

In Figs. 3 and 4 we show our scan results in the λ versus m_h plane and the λ versus m_a plane with m_h being the lightest CP -even Higgs boson mass and m_a the lighter CP -odd Higgs boson mass. From Fig. 3 one can learn that the upper bound of m_h increases with λ , which is

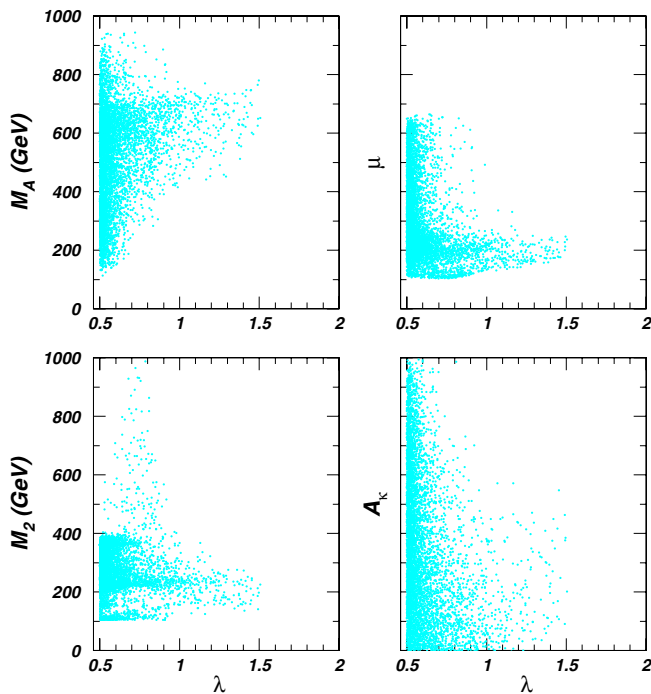


FIG. 2 (color online). Scatter plots of the NMSSM parameters satisfying all the constraints (1)–(9), displayed in different planes.

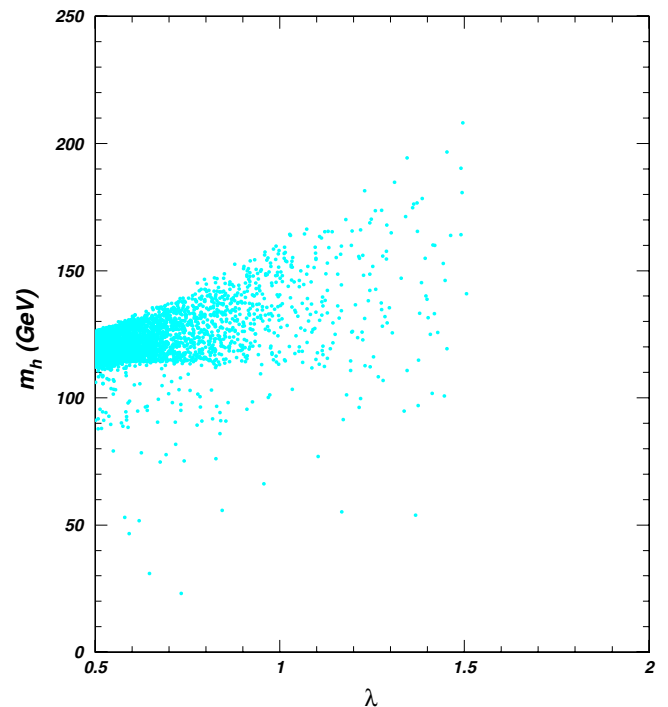


FIG. 3 (color online). Same as Fig. 2, but for λ versus the lightest CP -even Higgs boson mass m_h .

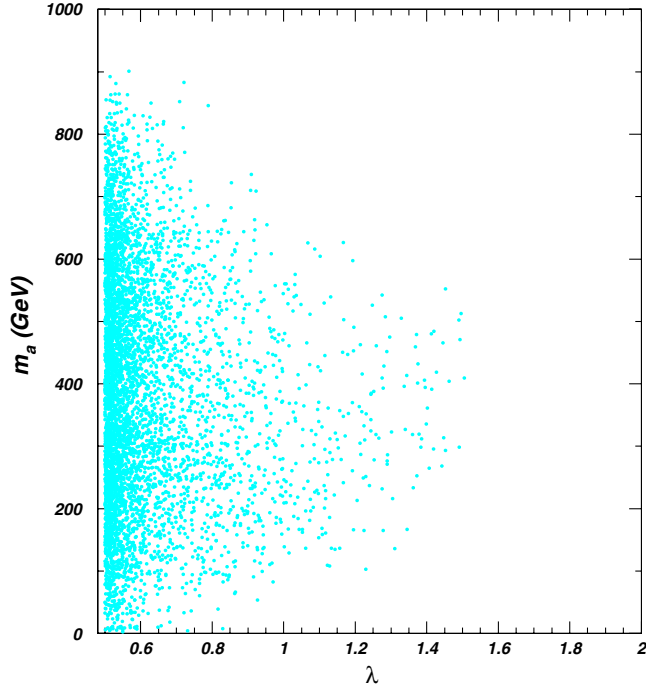


FIG. 4 (color online). Same as Fig. 2, but for λ versus the lightest CP -odd Higgs boson mass m_a .

expected from Eq. (1), and for $\lambda = 1.5$ the value of m_h can reach 210 GeV. From Fig. 4 one can learn that with the increase of λ , a super light CP -odd Higgs boson is gradually ruled out, and for $\lambda > 1$ it is bounded in the range $100 \text{ GeV} \lesssim m_a \lesssim 600 \text{ GeV}$. The properties of these Higgs bosons can be quite different from those in the MSSM, and their phenomenology at the LHC was discussed in [28].

Finally, in order to understand the mechanism used to reproduce the correct dark matter abundance, we consider the properties in the neutralino sector. In the NMSSM with large $\tan\beta$, the component of the lightest neutralino is either Higgsino dominant or b -ino dominant for a light mass below 80 GeV, but for a heavier mass it is b -ino dominant. In Fig. 5 we show our scan results in the plane of $m_{\tilde{\chi}_1^0}$ versus λ . We see that with the increase of λ , the upper bound on $m_{\tilde{\chi}_1^0}$ becomes stringent and eventually it is constrained in the range of 50–100 GeV. Regarding the next lightest neutralino $\tilde{\chi}_2^0$, we found that its mass is constrained in the range of 100–160 GeV for $\lambda > 1.2$. In order to figure out the annihilation mechanism of $\tilde{\chi}_1^0$ in providing for the dark matter relic density, we compare the masses of $\tilde{\chi}_2^0$ and a with $\tilde{\chi}_1^0$ in Fig. 6. This figure indicates that $\tilde{\chi}_2^0$ is significantly heavier than $\tilde{\chi}_1^0$. Since in our scan the slepton masses are fixed to 200 GeV, also significantly heavier than $\tilde{\chi}_1^0$, we conclude that the coannihilation of $\tilde{\chi}_1^0$ with $\tilde{\chi}_2^0$ or with a slepton is generally Boltzmann suppressed and plays an unimportant role in accounting for the dark matter relic density. Note that, as shown in Fig. 6, there are some samples around the funnel region $2m_{\tilde{\chi}_1^0} - m_a$, and in this

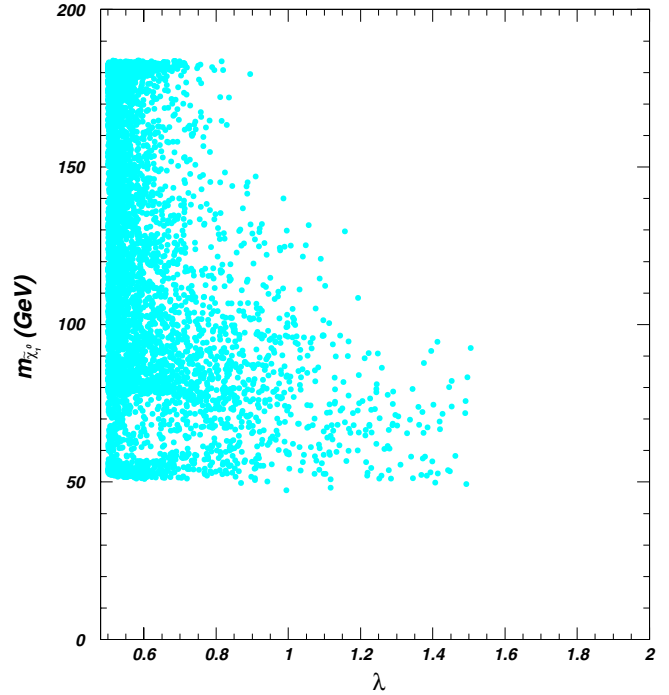


FIG. 5 (color online). Same as Fig. 2, but for the lightest neutralino mass $m_{\tilde{\chi}_1^0}$ versus λ .

case the annihilation of $\tilde{\chi}_1^0$ through the s -channel exchange of a light a becomes dominant [29].

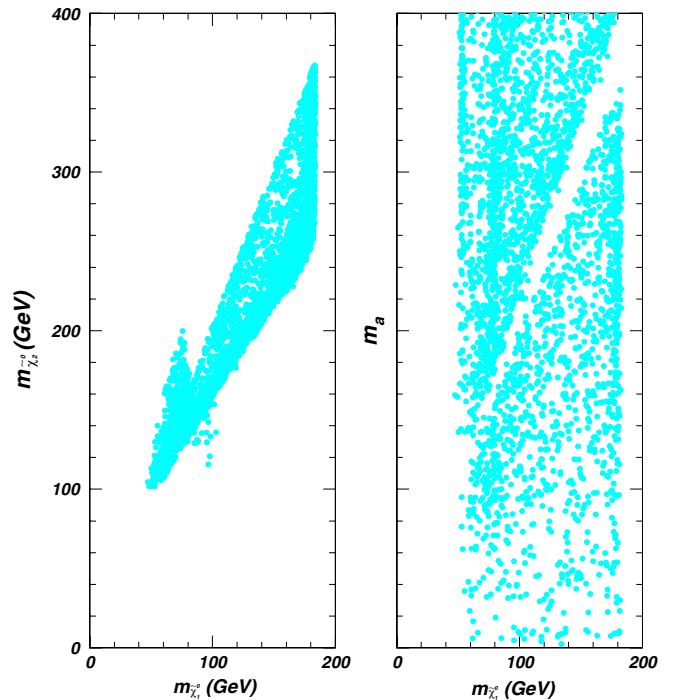


FIG. 6 (color online). Same as Fig. 2, but for $m_{\tilde{\chi}_2^0}$ and m_a versus $m_{\tilde{\chi}_1^0}$.

V. CONCLUSION

The NMSSM with a large λ is an attractive scenario since it can push up the upper bound on the SM-like Higgs boson mass to solve the little hierarchy problem. We examined the current experimental constraints on this scenario, which include the direct experimental bounds, the indirect constraints from precision electroweak measurements, the cosmic dark matter relic density, the muon anomalous magnetic moment, as well as the stability of the Higgs potential. Our results showed that for a large λ the parameter space is severely constrained. For example, for a smuon mass of 200 (500) GeV the parameter space with $\lambda \gtrsim 1.5(0.6)$ is excluded, and for $\lambda = 1$ the allowed ranges are 2.5–4 for $\tan\beta$, 400–800 GeV for M_A , 150–250 GeV for μ , 150–300 GeV for M_2 , and 0–600 GeV for A_κ .

Finally, we would like to point out that our conclusion may be qualitatively applicable to other NMSSM-like models such as the minimal nonminimal supersymmetric standard model (MNMSSM) [30], which has a similar

structure to the NMSSM and can be viewed as the low energy realization of the fat Higgs model [7]. For example, it has been pointed out that for any singlet extensions of the MSSM, regardless of the form of its superpotential, a large λ is always accompanied by a small $\tan\beta$ [8]. This property, as shown in our paper, can either limit the smuon mass or limit λ if we require the theory to explain the deviation of the muon anomalous magnetic moment. Another example is the constraint from dark matter. In the MNMSSM we expect that the constraint can limit the relevant parameters in a more stringent way than in the NMSSM since the neutralino sector in the MNMSSM is exactly the same as in the NMSSM but with fixed $\kappa = 0$ [31].

ACKNOWLEDGMENTS

This work was supported in part by the National Sciences and Engineering Research Council of Canada, and by the National Natural Science Foundation of China (NNSFC) under Grant No. 10505007, No. 10725526, and No. 10635030.

-
- [1] H.E. Haber and G.L. Kane, Phys. Rep. **117**, 75 (1985); J.F. Gunion and H.E. Haber, Nucl. Phys. **B272**, 1 (1986); **B402**, 567(E) (1993).
- [2] J.E. Kim and H.P. Nilles, Phys. Lett. **138B**, 150 (1984).
- [3] J.R. Ellis, J.F. Gunion, H.E. Haber, L. Roszkowski, and F. Zwirner, Phys. Rev. D **39**, 844 (1989); M. Drees, Int. J. Mod. Phys. A **4**, 3635 (1989); U. Ellwanger, M. Rausch de Traubenberg, and C.A. Savoy, Phys. Lett. B **315**, 331 (1993); Nucl. Phys. **B492**, 21 (1997); S.F. King and P.L. White, Phys. Rev. D **52**, 4183 (1995); F. Franke and H. Fraas, Int. J. Mod. Phys. A **12**, 479 (1997); B.A. Dobrescu and K.T. Matchev, J. High Energy Phys. 09 (2000) 031.
- [4] R. Dermisek and J.F. Gunion, Phys. Rev. Lett. **95**, 041801 (2005); Phys. Rev. D **73**, 111701 (2006); **75**, 075019 (2007); **76**, 095006 (2007).
- [5] J.R. Espinosa and M. Quiros, Phys. Lett. B **279**, 92 (1992); **302**, 51 (1993).
- [6] D.J. Miller, R. Nevzorov, and P.M. Zerwas, Nucl. Phys. **B681**, 3 (2004).
- [7] R. Harnik, G.D. Kribs, D.T. Larson, and H. Murayama, Phys. Rev. D **70**, 015002 (2004); S. Chang, C. Kilic, and R. Mahbubani, Phys. Rev. D **71**, 015003 (2005); A. Birkedal, Z. Chacko, and Y. Nomura, Phys. Rev. D **71**, 015006 (2005); A. Delgado and T.M.P. Tait, J. High Energy Phys. 07 (2005) 023.
- [8] R. Barbieri, L.J. Hall, Y. Nomura, and V.S. Rychkov, Phys. Rev. D **75**, 035007 (2007).
- [9] V. Barger, P. Langacker, H.S. Lee, and G. Shaughnessy, Phys. Rev. D **73**, 115010 (2006); V. Barger, P. Langacker, and G. Shaughnessy, Phys. Rev. D **75**, 055013 (2007); Phys. Lett. B **644**, 361 (2007).
- [10] See U. Ellwanger, J.F. Gunion, and C. Hugonie, J. High Energy Phys. 02 (2005) 066; U. Ellwanger and C. Hugonie, Comput. Phys. Commun. **175**, 290 (2006).
- [11] J.P. Derendinger and C.A. Savoy, Nucl. Phys. **B237**, 307 (1984); N.K. Falck, Z. Phys. C **30**, 247 (1986); R.B. Nevzorov and M.A. Trusov, Yad. Fiz. **64**, 1589 (2001) [Phys. At. Nucl. **64**, 1513 (2001)].
- [12] W.M. Yao *et al.* (Particle Data Group), J. Phys. G **33**, 1 (2006).
- [13] S. Schael *et al.*, Eur. Phys. J. C **47**, 547 (2006).
- [14] C.L. Bennett *et al.*, Astrophys. J. Suppl. Ser. **148**, 1 (2003); D.N. Spergel *et al.*, Astrophys. J. Suppl. Ser. **148**, 175 (2003).
- [15] G. Belanger, F. Boudjema, C. Hugonie, A. Pukhov, and A. Semenov, J. Cosmol. Astropart. Phys. 09 (2005) 001; V. Barger, P. Langacker, and H.S. Lee, Phys. Lett. B **630**, 85 (2005).
- [16] G. Altarelli and R. Barbieri, Phys. Lett. B **253**, 161 (1991); G. Altarelli, R. Barbieri, and S. Jadach, Nucl. Phys. **B369**, 3 (1992); **B376**, 444(E) (1992); G. Altarelli, R. Barbieri, and F. Caravaglios, Nucl. Phys. **B405**, 3 (1993); Phys. Lett. B **314**, 357 (1993).
- [17] LEP and SLD Collaborations, Phys. Rep. **427**, 257 (2006).
- [18] J.J. Cao and J.M. Yang, arXiv:0810.0751.
- [19] For a recent review, see J.P. Miller, E. de Rafael, and B.L. Roberts, Rep. Prog. Phys. **70**, 795 (2007); D. Stockinger, arXiv:0710.2429.
- [20] F. Domingo and U. Ellwanger, J. High Energy Phys. 07 (2008) 079.
- [21] J.F. Gunion, arXiv:0808.2509.
- [22] See, for example, T. Ibrahim and P. Nath, Phys. Rev. D **62**, 015004 (2000); S.P. Martin and J.D. Wells, Phys. Rev. D **64**, 035003 (2001).

- [23] W. A. Bardeen, R. Gastmans, and B. Lautrup, Nucl. Phys. **B46**, 319 (1972); J. P. Leveille, Nucl. Phys. **B137**, 63 (1978); H. E. Haber, G. L. Kane, and T. Sterling, Nucl. Phys. **B161**, 493 (1979); E. D. Carlson, S. L. Glashow, and U. Sarid, Nucl. Phys. **B309**, 597 (1988); J. R. Primack and H. R. Quinn, Phys. Rev. D **6**, 3171 (1972).
- [24] D. Chang, W.-F. Chang, C.-H. Chou, and W.-Y. Keung, Phys. Rev. D **63**, 091301 (2001); K. Cheung, C. H. Chou, and O. C. W. Kong, Phys. Rev. D **64**, 111301 (2001); A. Arhrib and S. Baek, Phys. Rev. D **65**, 075002 (2002).
- [25] G. Hiller, Phys. Rev. D **70**, 034018 (2004); F. Domingo and U. Ellwanger, J. High Energy Phys. 12 (2007) 090; Z. Heng *et al.*, Phys. Rev. D **77**, 095012 (2008); R. N. Hodgkinson, Phys. Lett. B **665**, 219 (2008).
- [26] S. Heinemeyer, W. Hollik, and G. Weiglein, J. High Energy Phys. 06 (2000) 009.
- [27] G. P. Lepage, J. Comput. Phys. **27**, 192 (1978).
- [28] L. Cavicchia, R. Franceschini, and V. S. Rychkov, Phys. Rev. D **77**, 055006 (2008).
- [29] J. F. Gunion, D. Hooper, and B. McElrath, Phys. Rev. D **73**, 015011 (2006).
- [30] C. Panagiotakopoulos and K. Tamvakis, Phys. Lett. B **469**, 145 (1999).
- [31] A. Menon, D. E. Morrissey, and C. E. M. Wagner, Phys. Rev. D **70**, 035005 (2004).